OPEN

Impaired brain glucose metabolism in cirrhosis without overt hepatic encephalopathy: a retrospective ^{18}F-FDG PET/CT study

Weishan Zhang[a], Ning Ning[b], Xianjun Li[a], Miao Li[a], Xiaoyi Duan[a], Youmin Guo[a], Yaping Dang[a], Yan Li[a], Jungang Gao[a], Jiajun Ye[a] and Jian Yang[a,c]

Objectives: **There are subclinical neurologic deficits in cirrhotic patients without overt hepatic encephalopathy. We aimed to use ^{18}F-fluorodeoxyglucose PET/computed tomography to explore the impaired brain glucose metabolism of subclinical hepatic encephalopathy in cirrhosis.**

Methods: **Thirty-seven patients with hepatitis B virus-related cirrhosis without overt hepatic encephalopathy and 49 controls were enrolled in the study. The patients' Model for End-Stage Liver Disease scores were calculated. All participants underwent resting state ^{18}F-fluorodeoxyglucose PET/computed tomography. Between-group comparisons of brain PET/computed tomography data were conducted with two-sample *t*-tests and multivariate tests with Statistical Parametric Mapping 8 software.**

Results: **Most of the patients (30/37) had a Model for End-Stage Liver Disease score of less than 20. The patients and controls did not significantly differ in baseline characteristics, such as sex, age, plasma glucose level, smoking history or BMI, but they did significantly differ in blood uric acid level and serum levels of bilirubin, albumin, total protein, alkaline phosphatase, alanine aminotransferase and aspartate aminotransferase ($P < 0.0001$). Relative to brain glucose metabolism in the controls, that in the patients involved both hyper- and hypometabolic regions ($P < 0.001$). The relative hypometabolic regions included the parietal, occipital and limbic lobes, and the hypermetabolic regions included the hippocampus, parahippocampal gyri, right basal ganglia and circumventricular organs.**

Conclusion: **Patients with cirrhosis have characteristic patterns of brain glycometabolic impairment. ^{18}F-fluorodeoxyglucose PET/computed tomography may serve as a preclinical biomarker for brain damage in cirrhosis. *NeuroReport* 30: 776–782 Copyright © 2019 The Author(s). Published by Wolters Kluwer Health, Inc.**

NeuroReport 2019, **30**:776–782

Keywords: brain, cirrhosis, glycometabolism, PET

[a]Radiology Department, First Affiliated Hospital, Xi'an Jiaotong University, [b]Nuclear Medicine Department, Second Affiliated Hospital, Xi'an Jiaotong University, and [c]Department of Biomedical Engineering, the Key Laboratory of Biomedical Information Engineering, Ministry of Education, School of Life Science and Technology, Xi'an Jiaotong University, Xi'an, Shaanxi, People's Republic of China

Correspondence to Jian Yang, MD, First Affiliated Hospital, Xi'an Jiaotong University, Xi'an, Shaanxi 710061, People's Republic of China
Tel: 086-029-85323643; e-mail: cjr.yangjian@vip.163.com

Received 21 April 2019 **Accepted** 20 May 2019

Introduction

In end-stage liver diseases such as cirrhosis, toxic substances are inadequately detoxified. Toxic substances therefore reach the brain and alter its function, resulting in hepatic encephalopathy (HE). HE manifests as a spectrum of cognitive and motor abnormalities ranging from minimal deficits to coma. HE severity has traditionally been graded with the West Haven Criteria (WHC), which allow classification into two broad categories: covert HE (CHE) for WHC grades of 0–1 and overt HE (OHE) for WHC grades of 2–4 [1]. CHE lacks the recognizable clinical manifestations of OHE but is associated with mild cognitive, motor control and concentration/attention deficits [1,2]. CHE occurs in up to 53% of patients with cirrhosis [2] and is linked to worsened clinical outcomes [3,4]. One longitudinal study of patients with cirrhosis (mean follow-up length: 4.8 years) found that 16 out of 34 (47%) patients with CHE subsequently developed OHE, which suggests that the presence of CHE can predict the subsequent development of OHE [2].

However, no gold standard for diagnosing CHE exists, and the diagnosis is only possible through various combinations of specialized psychometric and neuropsychological examinations [5]. Although these measures are generally sensitive and reproducible, their application across populations is limited by the need for highly specialized personnel and specific equipment and the lack of standardization and validated translations [3]. Further work is necessary to develop an optimal and widely accepted diagnostic strategy for CHE [5]. Studies of patients with cirrhosis without OHE may elucidate the underlying pathophysiology and aid the development of accurate diagnostic strategies.

Many researchers have been using structural and functional neuroimaging techniques in attempts to identify

0959-4965 Copyright © 2019 The Author(s). Published by Wolters Kluwer Health, Inc. DOI: 10.1097/WNR.0000000000001284

early biomarkers of brain impairment in patients with cirrhosis without OHE. They have reported various brain structural and functional abnormalities such as increased T1-weighted MRI signal intensities in the globus pallidus [6], impairments in basal ganglia-thalamocortical circuits [7], elevated glutathione levels in visual and sensorimotor areas assessed with magnetic resonance spectroscopy [8], decreased myoinositol/creatine and choline/creatine ratios and increased glutamine/creatine and glutamate/creatine ratios [9] and reduced functional connectivity in the default-mode network [10]. In mean diffusivity and fractional anisotropy maps, some white matter regions (i.e. the bilateral frontal lobes, corpus callosum and parietal lobes) may distinguish patients with minimal HE from those without HE with 75.4%–92.3% classification accuracy [11]. PET [12,13] and single-photon emission computed tomography (SPECT) [14] techniques revealed altered cerebral blood flow (CBF) patterns in patients with cirrhosis.

Despite these efforts, neurologic dysfunctions in patients with cirrhosis remain poorly elucidated, and the cerebral abnormalities involved in HE remains unclear, especially at the molecular level. ^{18}F-fluorodeoxyglucose (^{18}F-FDG) PET/CT is an efficient early detection technique for brain disorders such as Alzheimer's disease and epilepsy [15–17]. The spatial distribution of FDG uptake significantly correlates with functional MRI–derived metrics such as regional homogeneity, the fractional amplitude of low-frequency fluctuations and degree of centrality maps [18,19]. Glucose metabolism imaging may provide comprehensive and complementary information for decoding cerebral functions and networks [20]. Consistent with the critical cerebrophysiological role of glucose metabolism, impaired glucose metabolism constitutes the pathophysiological basis for many brain disorders. Investigating brain glucose metabolism may therefore facilitate explorations of the mechanisms underlying neurologic dysfunctions and identify biomarkers for early-stage HE in patients with cirrhosis. In this study, we used ^{18}F-FDG PET/CT to test the hypothesis that patients with hepatitis B virus (HBV) related cirrhosis without OHE would exhibit abnormal brain glucose metabolism patterns.

Methods

Ethics statement

This single-center retrospective study complied with institutional guidelines and regulations and was subject to approval by the Ethics Committee of the first author's hospital. This study was conducted in accordance with the principles of the Declaration of Helsinki.

Study population

All participants' records and information were anonymized before analysis. The patients with cirrhosis underwent whole-body PET/CT for the following reasons: patients with alpha-fetoprotein elevation, undiagnosed liver lesions (the final diagnosis of benign lesions such as hepatic cyst or hemangioma) and patients with contraindications for enhanced CT or MRI examinations. The control group underwent whole-body PET/CT for cancer-screening. Informed consent was obtained from all individual participants in this study. From May 2015 to March 2017, 152 HBV-related cirrhotic patients without head trauma, mental illness, neurodegenerative disease (e.g. Alzheimer's disease and Parkinson's disease), hypo- or hyperthyroidism, renal failure, chronic heart disease, drug or alcohol dependence or a previous history of alcoholism were consecutively enrolled. Brain CT and PET/CT scans were conducted on all patients. We excluded patients with clinical OHE diagnoses or histories of OHE, which were based on the Spectrum of Neurocognitive Impairment in Cirrhosis classification system [1]. To rule out non-cirrhosis-related effects on the brain, our other exclusion criteria included primary or metastatic brain tumours, interventional therapy, stroke, diabetes and prior surgery. The control group comprised individuals without cirrhosis. Fifty-eight controls without histories of cardio-cerebral diseases, mental illness, drug or alcohol dependence or a history of alcoholism were consecutively enrolled. The exclusion criteria of the control group were the same as the patients. All the participants, including the patients and the controls, underwent whole-body PET/CT tumour-screening in our hospital and showed no evidence of a malignancy. This malignancy-free status was confirmed in follow-up visits 6 months after the PET/CT scans. We excluded individuals with fasting plasma glucose levels higher than 6.1 mM or poor-quality PET/CT images marked by head motion artefacts and blurred cerebral contours. Patients with incomplete clinical data or PET imaging data missing were also excluded.

Clinical assessment

The Model for End-Stage Liver Disease (MELD) was initially developed to predict survival in patients undergoing transjugular intrahepatic portosystemic shunt operations, and it has been recognized as a major contribution to hepatology [21]. MELD incorporates three widely available laboratory variables: the international normalized ratio, serum creatinine and serum bilirubin. We calculated MELD scores with the following formula: MELDscore = 9.57 × In(Creatinine, mg/dl) + 3.78 × In(bilirubin, mg/dl) + 11.2 × In(INR) + 6.43.

PET/computed tomography acquisition

All participants underwent resting-state ^{18}F-FDG PET/CT with a clinical PET/CT scanner (Philips GEMINI TF 64; Philips, Amsterdam, the Netherlands) after fasting for ≥8 hours. After plasma glucose levels were verified, participants were injected with 3.7 MBq ^{18}F-FDG per kilogram of body weight (~220–440 MBq) and then rested with their eyes open in a quiet, dimly lit room. They were asked to refrain from reading, listening to

music or talking during the uptake period. A separate whole-body PET/CT scan (from lower jaw to upper thigh) was performed for diagnosis before brain scan with the starting time of 40–60 minutes after the FDG injection. The brain scan consisted of a simultaneous CT scan and 5-minute PET scan. A fully three-dimensional brain model was reconstructed from the 90 PET scan slices (128 × 128 pixels; 2- × 2-mm pixel size, 4-mm slice thickness) via a line-of-response row-action maximum likelihood algorithm. The brain CT data, which were acquired with a 120-kV voltage, a 240-mA current, and a 5-mm slice thickness, were used for attenuation correction of the PET images.

Data processing

We used Statistical parametric mapping 8 (SPM8; Wellcome Department of Cognitive Neurology, Institute of Neurology, University College London) implemented in MATLAB 7 (The MathWorks, Natick, Massachusetts, USA) for image processing. PET images were interpolated to a 2 × 2 × 2 mm voxel size, spatially normalized to the standard PET template embedded in SPM8, adjusted to the Talairach stereoscopic brain atlas, and further smoothed with a Gaussian kernel with a 5-mm full-width at half-maximum.

Statistical analysis

The data of characteristics in patients and controls were expressed as mean and SD unless otherwise stated. Differences between groups were tested using independent-samples *t*-test or Pearson's chi-square test in SPSS13.0. A *P* value of less than 0.05 was considered statistically significant.

Using SPM, two-sample *t*-tests, adjusted for age, BMI, sex, blood glucose and acquisition time were performed to compare the brain glucose metabolism between patients with cirrhosis and the controls, and the global normalization was applied. We also performed a multivariate analysis with a general linear model to investigate the associations between brain glucose metabolisms and MELD scores. The results were visualized using xjView (http://www.alivelearn.net/xjview) toolbox, an automated coordinate-based Talairach and Montreal Neurological Institute labelling system and a viewing program for SPM. Clusters of at least 50 voxels with significant intergroup differences ($P < 0.001$, corrected for multiple comparisons via a family-wise error method) are reported.

Results

We consecutively enrolled 152 patients with HBV-related cirrhosis and 58 controls. Based on the exclusion criteria, we excluded 115 patients and nine controls (Fig. 1). This left 37 patients (mean age: 52; male/female: 25/12) and 49 controls (mean age: 51; male/female: 32/17) in our study.

The distributions of selected characteristics among the patients and controls are shown in Table 1. All participants were right-handed and of Han Chinese ethnicity. The median MELD score was 15 (range: 5–29), and most (30/37) had a score of <20. The two groups did not significantly differ in baseline characteristics such as sex ratio, age, plasma glucose level, smoking history, BMI and the starting time of PET/CT acquisition ($P > 0.05$), but they did significantly differ in blood uric acid level and serum levels of bilirubin, albumin, total protein, sodium, potassium, alkaline phosphatase, alanine aminotransferase and aspartate aminotransferase ($P < 0.0001$).

Fig. 1

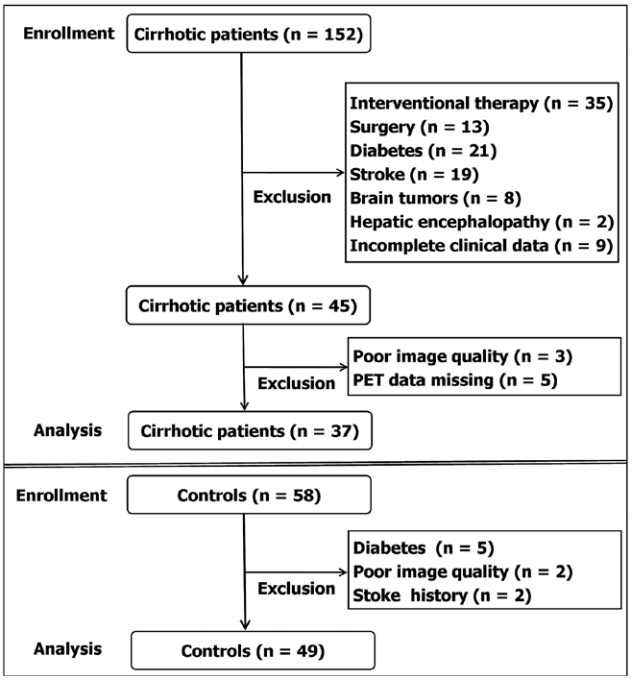

Flowchart of study population selection and the exclusion criteria.

A whole-brain analysis of glucose metabolism revealed regions of both increased and decreased uptake in the patients' brains (Fig. 2 and Table 2). In this study, SPM displayed a maximum intensity projection of the statistical map on a glass brain in three orthogonal planes, and the coloured figures provided additional quantitative information via the colour bar (Fig.2). The relative increased-uptake regions included the hippocampus, parahippocampal gyri, right basal ganglia and circumventricular organs, and the relative decreased-uptake regions included the parietal, occipital and limbic lobes. No regional glucose metabolism abnormalities were significantly associated with MELD scores.

Discussion

This study focussed on brain glucose metabolism patterns in patients with HBV-related cirrhosis without OHE. A whole-brain analysis of glycometabolism revealed clusters of both increased and decreased glucose uptake

Table 1 Distribution of characteristics in patients with cirrhosis and controls

	Patients (n = 37)[a]	Controls (n = 49)[a]	*P* value
Age (years)	52.2 ± 13.5 (28–80)	50.7 ± 7.4 (32–68)	0.53[b]
BMI (kg/m^2)	23.2 ± 2.8 (19–28)	24.3 ± 2.8 (20–28)	0.07[b]
Plasma glucose (mmol/L)	4.9 ± 0.9 (3.5–7.8)	4.9 ± 0.8 (3.6–7.2)	0.99[b]
Sex (male)	25 (67.6%)	32 (65.3%)	0.83[c]
Education (years)	9.4 ± 3.4 (6–19)	9.7 ± 3.6 (5–20)	0.73[b]
Smoker	18 (48.6%)	23(16.9%)	0.87[c]
Race (Chinese Han)	37 (100%)	49(100%)	-
Acquisition time (min)	52.8 ± 3.5 (45–60)	53.7 ± 3.7(45–60)	0.24[b]
MELD score	16 ± 6 (5–29)	-	-
Aetiology			
Hepatitis B virus	37(100%)	-	-
Bilirubin (μmol/L)	69.2 ± 108.4 (6.7–535.3)	11.5 ± 5.6 (3.8–25.1)	<0.0001[b]
Albumin (g/L)	35.3 ± 5.5 (25.0–44.0)	48.1 ± 3.3 (38.9–61.8)	<0.0001[b]
Serum total protein (g/L)	68.2 ± 7.2 (52.1–83.7)	75.5 ± 5.3 (59.5–80.8)	<0.0001[b]
Sodium (mmol/L)	135.0 ± 6.1 (121.0–147.8)	139.2 ± 3.7 (131.5–146.8)	<0.0001[b]
Potassium (mmol/L)	3.8 ± 0.7 (2.7–5.2)	4.5 ± 0.6 (3.2–5.3)	<0.0001[b]
Venous ammonia (μmol/L)	64.7 ± 25.1 (14.9–106.2)	-	-
ALP (U/L)	217.4 ± 197.0 (47.3–770.1)	58.5 ± 38.3 (35.5–100.8)	<0.0001[b]
ALT (U/L)	85.0 ± 71.1 (10.1–294.8)	22.7 ± 15.3 (8.5–42.7)	<0.0001[b]
AST (U/L)	118.0 ± 117.0 (15.0–605.1)	29.1 ± 11.3 (14.8–38.2)	<0.0001[b]
BUA (μmol/L)	296.1 ± 94.5 (134.1–546.3)	206.5 ± 51.3 (148.3–378.2)	<0.0001[b]
Prothrombin time (s)	15.1 ± 2.3 (11.6–22.0)	-	-
INR for prothrombin time	1.2 ± 0.2 (0.91–1.97)	-	-

Acquisition time, the starting time of PET/CT acquisition after ^{18}F-fluorodeoxyglucose (^{18}F-FDG) injection.
ALP, alkaline phosphatase; ALT, alanine aminotransferase; AST, aspartate aminotransferase; BUA, blood uric acid; INR, international normalized ratio; MELD, Model for End-Stage Liver Disease.
[a]Values are means ± SDs (range) or the number of subjects.
[b]Indicates independent-samples *t*-test results.
[c]Indicates Pearson's chi-square test results.

within the patients' brains. These results suggest that chronic liver disease is associated with impaired glucose metabolism in brain regions of attention, executive functions, visuospatial coordination and psychomotor functions.

PET and SPECT studies of CBF showed that CBF increases in the basal ganglia and decreases in the limbic cortex in patients with chronic liver disease. This observation could have been anticipated given the prominent and persistent neuropsychiatric symptoms associated with chronic liver disease [12,22]. Structural and functional MRI studies provide plentiful evidence of abnormalities in patients with minimal HE [23,24]. In Qi *et al.*'s study [24], the grey matter volumes of patients with minimal HE was increased in the thalamus and decreased in the frontal and temporal cortices, caudate, putamen, amygdala, paracentral lobule, anterior and middle cingulate cortices and supplementary motor area. Zafiris *et al.* [25] showed that minimal HE is associated with impaired coupling between visual judgment areas. Zhang *et al.* [7] concluded that widespread cortical and subcortical network connectivity changes, including weakening and strengthening of connections, were related to neuropsychological impairment in minimal HE. Our observation of hypo- and hypermetabolic brain regions is reasonably consistent with the results of previous studies in terms of structure and function, but they are not identical. This may be due to differences in the study participants and imaging methods.

In this study, extensive parts of the parietal, occipital and limbic lobes were located in the regions with significant FDG uptake reductions, and the calcarine, lingual and angular gyri covered abnormal spatial ranges. Parts of the parietal and occipital cortices are responsible for attention and visuospatial functions [26,27]. It has been suggested that patients with subclinical HE have abnormalities in areas responsible for attention, visuospatial coordination and psychomotor speed/reaction times [28]. The decreased regional FDG uptake in our study may be associated with dysfunctions in attentional and visuospatial abilities in patients with cirrhosis, and our findings support the hypothesis that the brain areas associated with these functions are selectively affected in cirrhotic patients without OHE. Lockwood *et al.* [29] reported that hypermetabolism was found in the visual associative regions based on the comparison between five patients with alcoholic cirrhosis and nine controls, which were different from our results. The different aetiologies of our participants may result in different patterns of cerebral glycometabolism, as it is reported that patients with alcoholic cirrhosis commonly had learning and memory deficits which were not evident in other aetiological cirrhosis, but the deficits in attention and concentration were not aetiologically specific [30].

On the other hand, we observed relative increased FDG uptake in the hippocampus, parahippocampal gyri, right basal ganglia and circumventricular organs. Several PET and SPECT studies consistently showed that glucose metabolism, ammonia metabolism and CBF were increased in the basal ganglia, parahippocampal gyri and lingual gyrus in patients with cirrhosis [13,29,31]. D'Mello *et al.* [32] examined a mouse model of inflammatory liver

Fig. 2

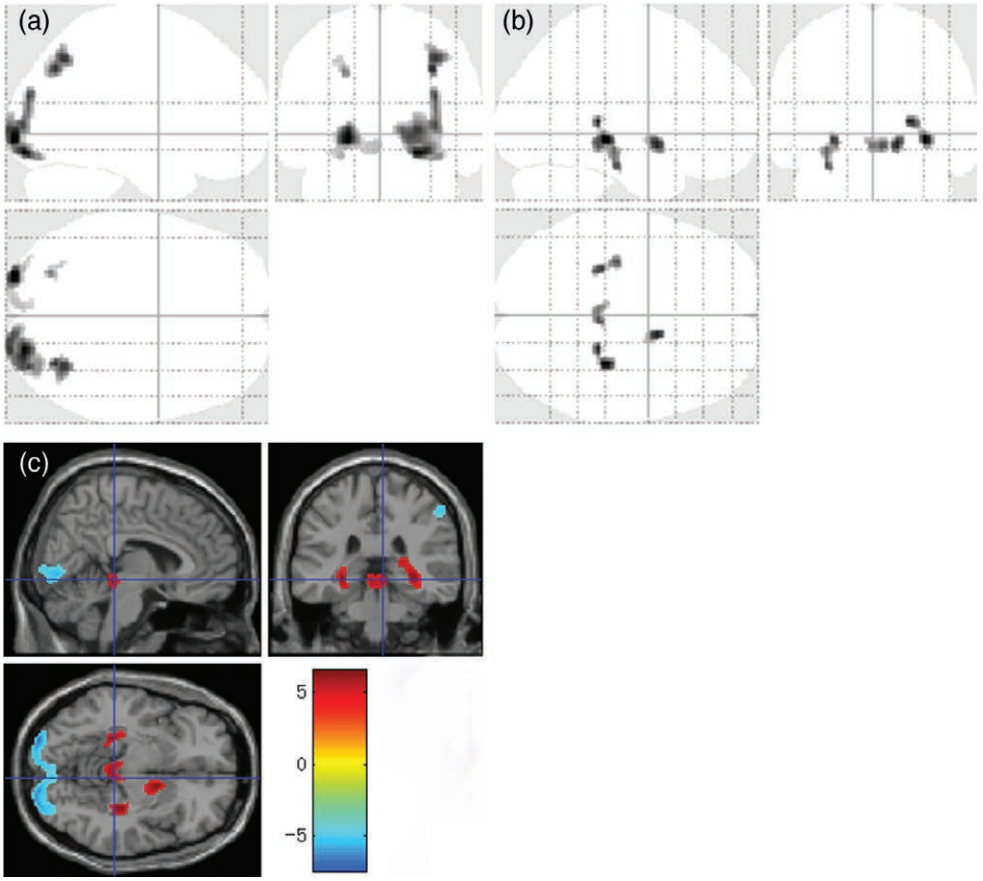

Both decreased and increased brain FDG uptake in patients with cirrhosis. SPM 'glass brain' regions with (a) decreased glucose uptake and (b) increased glucose uptake. (c) PET findings from a voxel-based statistical *t* image overlaid on a magnetic resonance image show clusters of abnormal glucose metabolism in patients with cirrhosis ($P < 0.001$ relative to controls; >50 continuous voxels; corrected for multiple comparisons via a family-wise error method). The colored bar represents *t*-values, and the display threshold is set at $|t| > 5.2$. SPM, statistical parametric mapping.

injury and confirmed that activated monocytes infiltrated the basal ganglia, hippocampus and motor cortex and that activated microglia clustered in the periventricular regions and areas close to blood vessels. The accumulation and activation of monocytes and microglia in these brain regions may induce increased glucose uptake. We speculate that increases in ^{18}F-FDG uptake are partially associated with these inflammatory cells.

As for the mechanism of the influences by liver cirrhosis on brain function, the reported liver-to-brain signalling mechanisms include hyperammonemia and systemic inflammation, which cause activation of microglia, neuroinflammation and neuronal dysfunction [33]. In the subclinical HE, the patients with cirrhosis manifest as a spectrum of dysarthria, ataxia, flapping tremor, disorientation and obvious slow mental processing [34], and the minimal brain function changes can be characterized by the decreased/increased ^{18}F-FDG uptake via brain PET/CT imaging. The findings in our study suggest a role for neuro imaging technique for the assessment of regional metabolic alterations in relation to brain dysfunction in cirrhotic patients without OHE.

It has been suggested that the MELD is a more ideal and objective survival model in patients with end-stage liver disease than Child-Turcotte-Pugh [21], and the MELD score was used to prioritize liver allocation in the US as of 27 February 2002. The calculation of the MELD score does not require 'subjective' assessment of HE. In our study, 30 of 37 the cirrhotic patients had a score of <20, and it was observed no regional glucose uptake was significantly associated with MELD score. Yoo *et al.* [35] reported that the MELD score did not correlate well with severity of HE, and the scores were not significantly different in patients with or without HE. Our results may be a kind of supplement to Yoo's study from the perspective of molecular imaging.

Our study has several limitations. First, we could not adequately assess the correspondence of cerebral glucose metabolism with the participants' results on

Table 2 Comparison of normalized brain glucose uptake in 37 cirrhotic patients and 49 controls

			Peak intensity		Peak MNI coordinates		
Cluster size (voxels)[a]	Brain region	Size (voxels)	*t*	Cohen's *d*	x	y	z
336	Hippocapus_L[b]	171	6.1	1.33	−28	−32	−6
	ParaHippocampal_L	100					
415	Hippocapus_R[b]	243	6.5	1.42	32	−30	−6
	ParaHippocampal_R	74					
175	Putamen_R[b]	21	6.3	1.37	14	4	−8
	Pallidum_R	66					
198	Brainstem_R[b]	98	6.0	1.31	4	−34	−10
	Brainstem_L	92					
	Vermis_3	49					
2357	Occipital_Mid_R[b]	428	−7.4	−1.61	−24	−98	−4
	Occipital_Mid_L	179					
	Calcarine_L	335					
	Lingual_R	334					
	Calcarine_R	273					
	Lingual_L	184					
	Occipital_Inf_R	354					
	Occipital_Inf_L	144					
100	Frontal_Inf_Oper_R[b]	78	−6.6	−1.44	54	8	22
384	Parietal_Inf_L[b]	245	−6.2	−1.35	−44	−48	46
	Occipital_Mid_L	66					
82	Precentral_L[b]	70	−6.1	−1.33	−42	6	32
378	Occipital_Sup_R[b]	40	−6.8	−1.48	32	−70	40
	Angular_R	209					
	Parietal_Sup_R	63					
294	SupraMarginal_R[b]	114	−5.8	−1.26	56	−26	42
	Parietal_Inf_R	151					

Brain regions are classified according to xjView definitions ($P < 0.001$ relative to controls; corrected for multiple comparisons via a family-wise error method).
MNI, Montreal Neurological Institute.
[a]Cluster size is indicated by the K value, which represents the number of significant voxels in the particular cluster.
[b]The indicated region is the cluster's peak region.

neuropsychiatric tests, such as the number connection test, block design test or digit symbol test. Second, our retrospective study population included patients with cirrhosis without OHE, so it might have included both patients with CHE, which is minimal HE with Grade I changes according to the WHC, and unimpaired patients who had no clinical, neurophysiological, or neuropsychometric changes. Distinguishing between these two groups is very important in clinic, and future prospective studies would examine how they can be distinguished. Third, we enrolled the subjects with a single aetiology of HBV-related cirrhosis, and we thought it could avoid the bias caused by different aetiologies. However, exploring the characteristic brain metabolism of different aetiologies needs further study in the future. Moreover, analysing the brain metabolic pattern with the follow-up of the patients may provide important clinical value, considering that patients of brain glucose metabolism is more likely to develop into OHE. This preliminary study explored disordered brain glycometabolism in patients with HBV-related cirrhosis but establishing the clinical importance of our findings necessitates prospective studies with large samples and multidisciplinary collaborative approaches, and brain PET studies using specific radiopharmaceutical markers would likely be useful in such future studies.

Conclusions

Our study maps the glucose metabolism impairments in the brains of HBV-related cirrhosis patients without OHE, and the combination of increased and decreased cerebral glucose metabolism represents the anatomical and pathophysiological bases for the expression of subclinical HE. Because these deficits are not clinically obvious, our findings have important implications for the management of CHE patients with chronic HBV-related cirrhosis. ^{18}F-FDG PET/CT may serve as a promising biomarker for the presence and progression of brain damage in cirrhotic patients.

Acknowledgements

This work was supported by the National Key Research and Development Program of China (2016YFC0100300), National Natural Science Foundation of China (No.81171317, 81471631), the 2011 New Century Excellent Talent Support Plan of Ministry of Education of China (NCET-11–0438), the Clinical Research Award of the First Affiliated Hospital of Xi'an Jiaotong University (No. XJTU1AF-CRF-2015-004) and Fund of the First Affiliated Hospital of Xi'an Jiaotong University (2014YK22). The funders had no role in study design, data collection and analysis, decision to publish or preparation of the manuscript.

Conceptualization, funding acquisition and writing-review and editing: J.Y. and W.S.Z. Resources and data analysis: N.N., ML., Y.L., J.G.G. and J.J.Y. Methodology: W.S.Z., X.J.L., X.Y.D., Y.M.G. and Y.P.D. Writing-original

draft: W.S.Z. and N.N. Supervision and validation: J.Y., Y.M.G. and Y.P.D.

Conflicts of interest

There are no conflicts of interest.

References

1 Bajaj JS, Cordoba J, Mullen KD, Amodio P, Shawcross DL, Butterworth RF, Morgan MY; International Society for Hepatic Encephalopathy and Nitrogen Metabolism (ISHEN). Review article: the design of clinical trials in hepatic encephalopathy–an International Society for Hepatic Encephalopathy and Nitrogen Metabolism (ISHEN) consensus statement. *Aliment Pharmacol Ther* 2011; **33**:739–747.

2 Romero-Gómez M, Boza F, García-Valdecasas MS, García E, Aguilar-Reina J. Subclinical hepatic encephalopathy predicts the development of overt hepatic encephalopathy. *Am J Gastroenterol* 2001; **96**:2718–2723.

3 Bajaj JS, Wade JB, Sanyal AJ. Spectrum of neurocognitive impairment in cirrhosis: implications for the assessment of hepatic encephalopathy. *Hepatology* 2009; **50**:2014–2021.

4 Bajaj JS, Pinkerton SD, Sanyal AJ, Heuman DM. Diagnosis and treatment of minimal hepatic encephalopathy to prevent motor vehicle accidents: a cost-effectiveness analysis. *Hepatology* 2012; **55**:1164–1171.

5 NeSmith M, Ahn J, Flamm SL. Contemporary understanding and management of overt and covert hepatic encephalopathy. *Gastroenterol Hepatol (N Y)* 2016; **12**:91–100.

6 Kulisevsky J, Pujol J, Deus J, Junqué C, Balanzó J, Avila A, Capdevila A. Persistence of MRI hyperintensity of the globus pallidus in cirrhotic patients: a 2-year follow-up study. *Neurology* 1995; **45**:995–997.

7 Zhang LJ, Zheng G, Zhang L, Zhong J, Wu S, Qi R, *et al*. Altered brain functional connectivity in patients with cirrhosis and minimal hepatic encephalopathy: a functional MR imaging study. *Radiology* 2012; **265**:528–536.

8 Oeltzschner G, Butz M, Wickrath F, Wittsack HJ, Schnitzler A. Covert hepatic encephalopathy: elevated total glutathione and absence of brain water content changes. *Metab Brain Dis* 2016; **31**:517–527.

9 Zhang LJ, Zhong J, Lu GM. Multimodality MR imaging findings of low-grade brain edema in hepatic encephalopathy. *AJNR Am J Neuroradiol* 2013; **34**:707–715.

10 Zhang L, Qi R, Wu S, Zhong J, Zhong Y, Zhang Z, *et al*. Brain default-mode network abnormalities in hepatic encephalopathy: a resting-state functional MRI study. *Hum Brain Mapp* 2012; **33**:1384–1392.

11 Chen HJ, Chen R, Yang M, Teng GJ, Herskovits EH. Identification of minimal hepatic encephalopathy in patients with cirrhosis based on white matter imaging and bayesian data mining. *AJNR Am J Neuroradiol* 2015; **36**:481–487.

12 O'Carroll RE, Hayes PC, Ebmeier KP, Dougall N, Murray C, Best JJ, *et al*. Regional cerebral blood flow and cognitive function in patients with chronic liver disease. *Lancet* 1991; **337**:1250–1253.

13 Ahl B, Weissenborn K, van den Hoff J, Fischer-Wasels D, Köstler H, Hecker H, Burchert W. Regional differences in cerebral blood flow and cerebral ammonia metabolism in patients with cirrhosis. *Hepatology* 2004; **40**:73–79.

14 Catafau AM, Kulisevsky J, Bernà L, Pujol J, Martin JC, Otermin P, *et al*. Relationship between cerebral perfusion in frontal-limbic-basal ganglia circuits and neuropsychologic impairment in patients with subclinical hepatic encephalopathy. *J Nucl Med* 2000; **41**:405–410.

15 Smailagic N, Vacante M, Hyde C, Martin S, Ukoumunne O, Sachpekidis C. ^{18}F-FDG PET for the early diagnosis of alzheimer's disease dementia and other dementias in people with mild cognitive impairment (MCI). *Cochrane Database Syst Rev* 2015; **1**:CD010632.

16 Herholz K. Use of FDG PET as an imaging biomarker in clinical trials of Alzheimer's disease. *Biomark Med* 2012; **6**:431–439.

17 Uijl SG, Leijten FS, Arends JB, Parra J, van Huffelen AC, Moons KG. The added value of [18F]-fluoro-D-deoxyglucose positron emission tomography in screening for temporal lobe epilepsy surgery. *Epilepsia* 2007; **48**:2121–2129.

18 Aiello M, Salvatore E, Cachia A, Pappatà S, Cavaliere C, Prinster A, *et al*. Relationship between simultaneously acquired resting-state regional cerebral glucose metabolism and functional MRI: a PET/MR hybrid scanner study. *Neuroimage* 2015; **113**:111–121.

19 Tomasi D, Wang GJ, Volkow ND. Energetic cost of brain functional connectivity. *Proc Natl Acad Sci U S A* 2013; **110**:13642–13647.

20 Wehrl HF, Hossain M, Lankes K, Liu CC, Bezrukov I, Martirosian P, *et al*. Simultaneous PET-MRI reveals brain function in activated and resting state on metabolic, hemodynamic and multiple temporal scales. *Nat Med* 2013; **19**:1184–1189.

21 Kamath PS, Kim WR; Advanced Liver Disease Study Group. The Model for End-Stage Liver Disease (MELD). *Hepatology* 2007; **45**:797–805.

22 Iversen P, Sørensen M, Bak LK, Waagepetersen HS, Vafaee MS, Borghammer P, *et al*. Low cerebral oxygen consumption and blood flow in patients with cirrhosis and an acute episode of hepatic encephalopathy. *Gastroenterology* 2009; **136**:863–871.

23 Zhang XD, Zhang LJ, Wu SY, Lu GM. Multimodality magnetic resonance imaging in hepatic encephalopathy: an update. *World J Gastroenterol* 2014; **20**:11262–11272.

24 Qi R, Zhang LJ, Zhong J, Zhu T, Zhang Z, Xu C, *et al*. Grey and white matter abnormalities in minimal hepatic encephalopathy: a study combining voxel-based morphometry and tract-based spatial statistics. *Eur Radiol* 2013; **23**:3370–3378.

25 Zafiris O, Kircheis G, Rood HA, Boers F, Häussinger D, Zilles K. Neural mechanism underlying impaired visual judgement in the dysmetabolic brain: an fmri study. *Neuroimage* 2004; **22**:541–552.

26 Petersen SE, Posner MI. The attention system of the human brain: 20 years after. *Annu Rev Neurosci* 2012; **35**:73–89.

27 Shomstein S, Lee J, Behrmann M. Top-down and bottom-up attentional guidance: investigating the role of the dorsal and ventral parietal cortices. *Exp Brain Res* 2010; **206**:197–208.

28 Córdoba J. New assessment of hepatic encephalopathy. *J Hepatol* 2011; **54**:1030–1040.

29 Lockwood AH, Murphy BW, Donnelly KZ, Mahl TC, Perini S. Positron-emission tomographic localization of abnormalities of brain metabolism in patients with minimal hepatic encephalopathy. *Hepatology* 1993; **18**:1061–1068.

30 Tarter RE, Hegedus AM, Van Thiel DH, Edwards N, Schade RR. Neurobehavioral correlates of cholestatic and hepatocellular disease: differentiation according to disease specific characteristics and severity of the identified cerebral dysfunction. *Int J Neurosci* 1987; **32**:901–910.

31 Lockwood AH, Yap EW, Wong WH. Cerebral ammonia metabolism in patients with severe liver disease and minimal hepatic encephalopathy. *J Cereb Blood Flow Metab* 1991; **11**:337–341.

32 D'Mello C, Le T, Swain MG. Cerebral microglia recruit monocytes into the brain in response to tumor necrosis factoralpha signaling during peripheral organ inflammation. *J Neurosci* 2009; **29**:2089–2102.

33 Butterworth RF. The liver-brain axis in liver failure: neuroinflammation and encephalopathy. *Nat Rev Gastroenterol Hepatol* 2013; **10**:522–528.

34 Ortiz M, JacasC, CórdobaJ. Minimal hepatic encephalopathy: diagnosis, clinical significance and recommendations. *J Hepatol* 2005; **42**:S45–S53.

35 Yoo HY, Edwin D, Thuluvath PJ. Relationship of the Model for End-Stage Liver Disease (MELD) scale to hepatic encephalopathy, as defined by electroencephalography and neuropsychometric testing, and ascites. *Am J Gastroenterol* 2003; **98**:1395–1399.